NASA TECHNICAL NOTE

NASA TN D-6558
$C.1$

NASA TN D-6558

EFFECTS OF LOADING SEQUENCE
FOR NOTCHED SPECIMENS UNDER
HIGH-LOW TWO-STEP FATIGUE LOADING

by John H. Crews, Jr.

Langley Research Center

Hampton, Va. 23365

NATIONAL AERONAUTICS AND SPACE ADMINISTRATION • WASHINGTON, D. C. • NOVEMBER 1971

1. Report No. NASA TN D-6558	2. Government Accession No.	3. Recipient's Catalog No.
4. Title and Subtitle EFFECTS OF LOADING SEQUENCE FOR NOTCHED SPECIMENS UNDER HIGH-LOW TWO-STEP FATIGUE LOADING		5. Report Date November 1971
		6. Performing Organization Code
7. Author(s) John H. Crews, Jr.		8. Performing Organization Report No. L-7915
9. Performing Organization Name and Address NASA Langley Research Center Hampton, Va. 23365		10. Work Unit No. 134-03-21-01
		11. Contract or Grant No.
12. Sponsoring Agency Name and Address National Aeronautics and Space Administration Washington, D.C. 20546		13. Type of Report and Period Covered Technical Note
		14. Sponsoring Agency Code

15. Supplementary Notes

16. Abstract

The effects of loading sequence on crack-initiation period have been investigated for notched aluminum-alloy specimens under high-low two-step loading with special emphasis on local cyclic stresses and strains at the notch root. Local stress and strain were determined by a procedure based on an equation proposed by Neuber which relates elastoplastic stress and strain at a notch. Local stress and strain were also measured experimentally to verify the Neuber equation.

The effects of initial high load on the crack-initiation periods were demonstrated with notched specimens and were simulated in unnotched specimens fatigue tested with local stress sequences. An analysis of the results indicated that sequence effects were not caused solely by local residual stresses, as is usually assumed; the existence of a damaging effect, resulting from the high local strain cycles, was demonstrated. The sequence effects observed with notched specimens were interpreted as the combined result of residual stresses and high local strain cycles.

17. Key Words (Suggested by Author(s)) Crack initiation Fatigue Notched specimen Plasticity Two-step loading Loading-sequence effect Local stress and strain	18. Distribution Statement Unclassified – Unlimited

19. Security Classif. (of this report) Unclassified	20. Security Classif. (of this page) Unclassified	21. No. of Pages 25	22. Price* $3.00

EFFECTS OF LOADING SEQUENCE FOR NOTCHED SPECIMENS
UNDER HIGH-LOW TWO-STEP FATIGUE LOADING

By John H. Crews, Jr.
Langley Research Center

SUMMARY

The effects of loading sequence on crack-initiation period have been investigated for notched aluminum-alloy specimens under high-low two-step loading with special emphasis on local cyclic stresses and strains at the notch root. Local stress and strain were determined by a procedure based on an equation proposed by Neuber which relates elastoplastic stress and strain at a notch. Local stress and strain were also measured experimentally to verify the Neuber equation.

The effects of initial high load on the crack-initiation periods were demonstrated with notched specimens and were simulated in unnotched specimens fatigue tested with local stress sequences. An analysis of the results indicated that sequence effects were not caused solely by local residual stresses, as is usually assumed; the existence of a damaging effect, resulting from the high local-strain cycles, was demonstrated. The sequence effects observed with notched specimens were interpreted as the combined result of residual stresses and high local strain cycles.

INTRODUCTION

Cumulative-damage calculations for notched specimens are frequently based on the linear-damage rule (ref. 1), but results too often are unsatisfactory. Errors are often attributed to residual stresses caused by the high loads in a loading sequence. Numerous studies of loading-sequence effects show general trends but offer only qualitative explanations for these trends. (See, for example, refs. 2 to 4.) Specific knowledge of local stress and strain, necessary for accurate fatigue-life predictions, is lacking.

The present investigation was undertaken to analyze the effects of loading sequence in terms of the corresponding local stress-strain sequence at a notch. The case studied was that of high-low two-step loading on a sheet specimen containing a circular hole (herein referred to as a notched specimen). Local stress-strain sequences were determined by an approximate procedure (ref. 5), based on an equation proposed by Neuber (ref. 6), and, for comparison, were also found by a direct-measurement procedure (ref. 7). These stress-strain sequences were applied to unnotched specimens to simulate the

crack-initiation behavior at the notch. The relative contributions of residual stress and initial high local strain were then analyzed by comparing lives from notched specimens with those from the unnotched specimens which were used to simulate behavior at the notch.

A new testing system was used for the direct measurement of local stress and strain. The system involves strain-coupled servocontrol to test simultaneously a notched specimen and an unnotched companion specimen. A brief description of the system is included in an appendix.

SYMBOLS

The units used for the physical quantities defined in this paper are given both in the International System of Units (SI) (ref. 8) and in the U.S. Customary Units. The measurements and calculations were made in U.S. Customary Units.

E Young's modulus, MN/m^2 (ksi)

K_T theoretical elastic stress-concentration factor

K_ϵ strain-concentration factor

K_σ stress-concentration factor

N number of cycles

N_c crack-propagation period, cycles

N_f total fatigue life, cycles

N_o crack-initiation period, cycles

S nominal net-section stress, MN/m^2 (ksi)

S_{max} maximum nominal net-section stress, MN/m^2 (ksi)

ΔS_i range of nominal net-section stress for ith monotonic load excursion, MN/m^2 (ksi)

ϵ local strain

2

$\Delta \epsilon_i$ range of local strain corresponding to ΔS_i

σ local stress, MN/m^2 (ksi)

$\Delta \sigma_i$ range of local stress corresponding to ΔS_i, MN/m^2 (ksi)

PROCEDURES

The study was conducted in three phases: (1) local cyclic stresses and strains were determined for a notched specimen under high-low loading; (2) the effects of initial high load on the crack-initiation period at the low load were demonstrated by fatigue tests with notched specimens; and (3) these sequence effects were then simulated by the fatigue testing of unnotched specimens by using local stress sequences determined for the notched specimen. The simulation of sequence effects provided data for evaluating the separate contributions of local residual stress and high local strains produced by the high loading.

Specimens and Loading Sequences

The notched specimen is shown in figure 1(a). When loaded uniaxially, it has an elastic-stress concentration of 2.57, which can be obtained from reference 9, with the two points of maximum stress on the transverse axis at the boundary of the hole. Attention was focused on these fatigue-critical points, and the conditions at these points are referred to as "local" conditions.

The unnotched specimen configuration is shown in figure 1(b). It was used both in the study of local stress-strain behavior and in the simulation of sequence effects. All unnotched and notched specimens were machined from one sheet of 2024-T3 aluminum alloy, 3.96 mm (0.156 inch) thick.

Loading sequences for the notched specimens are shown in figure 2. The constant-amplitude sequence in figure 2(a) served as a reference case to establish the fatigue behavior in the absence of initial high loading. Each of the high-low loading sequences, figures 2(b) and 2(c), consisted of 10 cycles of completely reversed high loading followed by zero-to-tension loading at a lower level equal to that of the reference case. The high loading was selected to produce reversed local plasticity at the notch; it was repeated for 10 cycles to stabilize local strain hardening. (See ref. 10.) The subsequent low loading was selected to produce elastic cyclic behavior at the stress concentration, so that the local residual stress would not decay during the fatigue cycling. The essential difference between the two high-low sequences is the sense in which the high loading was terminated. In figure 2(b), the high loads were terminated after a tensile peak load, and a compressive residual stress was produced; this sequence is called "beneficial initial loading." In

3

figure 2(c), high loading was terminated after a compressive peak load, and a tensile residual stress was produced; this sequence is called "detrimental initial loading."

Determination of Local Stress and Strain

Local stress and strain were determined by a combined theoretical and experimental procedure called the Neuber procedure (ref. 5). Maximum and minimum local stress-strain conditions were calculated for each load cycle by using an equation proposed by Neuber (ref. 6), $K_T^2 = K_\sigma K_\epsilon$, where K_T is the theoretical elastic stress-concentration factor, and K_σ and K_ϵ are the stress- and strain-concentration factors altered by local yielding. An unnotched specimen was cyclically loaded between the limiting conditions to establish the local stress-strain history for the notched specimen, as explained in appendix A.

To evaluate the accuracy of the Neuber procedure, local stress and strain were measured directly by the companion-specimen procedure. (See ref. 10.) In this experimental procedure, local maximum and minimum cyclic strains at the notch root were measured with small strain gages. Unnotched specimens then were cyclically loaded between these strains to determine the corresponding local stresses. A strain-coupled system was developed which enabled simultaneous testing of the notched and unnotched companion specimens. The procedure and a description of the system are presented in appendix B.

The effects of high initial loads on local stress and strain were evaluated by comparing the local stress-strain behavior for each type of high-low loading with that for the reference case of no initial high loading. Since local stresses and strains for the reference case were elastic, they were calculated by using the elastic stress-concentration factor for the notched specimen.

Measurement of Sequence Effects

For the two-step loading used in this study, the sequence effects are caused by changes in the local stress-strain behavior near the notch. Consequently, the sequence effects are operative primarily during the crack-initiation period of fatigue life. For this reason, sequence effects were expressed in terms of crack-initiation periods.

During the tests, fatigue cracks were detected by observing the edge of the hole with a microscope. The crack-initiation period N_0 was arbitrarily defined as the number of cycles required to produce a 0.76-mm-long (0.03-inch) crack. In many tests, however, cracks extended beyond this length before they were detected. For these tests, N_0 was found by subtracting the crack-propagation period beyond a crack length of 0.76 mm (0.03 inch) N_c from the total fatigue life N_f. The crack-propagation period was assumed to be constant for each loading sequence and was determined from tests in

which the crack was detected before reaching a length of 0.76 mm (0.03 inch). Errors resulting from this procedure were small because the crack-propagation lives were less than 10 percent of the total fatigue life for all three loading sequences.

Separation of the Effects of Residual Stress and High Local Strain

In reference 11, it was suggested that high-stress cycles may produce microscopic cracks which grow readily under subsequent lower stresses and thus reduce fatigue life. This damaging effect was demonstrated in reference 12 by fatigue tests on unnotched specimens with initial-strain cycles. Since the test material and local strain levels in the present study were similar to those in reference 12, the loading-sequence effects were expected to be caused by the combined result of this high initial strain effect and the residual stress effects.

The initial strain effect and the residual stress effects were separated by means of three series of fatigue tests in which unnotched specimens were loaded to stress levels equal to those calculated for the notch root by the Neuber procedure. By this approach, unnotched specimens were used to simulate the crack-initiation behavior of notched specimens. In the first series, unnotched specimens were tested under the complete local stress sequence (determined for each type of two-step loading); thereby, the combined result of the initial strain and residual stress effects was simulated. In the second series, unnotched specimens were cyclically loaded only under that portion of the local stress sequence corresponding to the low level in each type of two-step loading; that is, the high initial strains were not included in the simulation. The second series of tests therefore simulated only the residual stress effects. In the third series, unnotched specimens were tested under the local stress (determined for the case of no initial loading on the notched specimen) to establish a reference life.

Results from the three series of tests were compared to separate the effects of residual stress and local strain cycles.

RESULTS AND DISCUSSION

Effects of Initial High Loads on Local Stress and Strain

For convenience, local stress and strain results are presented in terms of maximum and minimum values in a load cycle. Stresses and strains will be presented and discussed separately.

Local stresses.- Local stresses, determined by both the Neuber and the companion-specimen procedures, are presented in figure 3 for the first 50 cycles of the beneficial initial loading sequence. For the 10 cycles of high loading, yielding occurred in both tension and compression and therefore produced half-cycle and full-cycle residual stresses.

Because of the cyclic strain-hardening behavior of 2024-T3 aluminum alloy, the local-stress range increased and approached a stabilized value. Results in reference 7 show that stabilization was virtually complete by the 10th cycle.

Since the local conditions were elastic for the low-level loading, the local stress range was $S_{max}K_T$, which for the present case was 355 MN/m^2 (51.4 ksi). This elastic local stress, corresponding to the second level of loading, cycled between a minimum value of -208 MN/m^2 (-30.1 ksi) (the half-cycle residual stress for the 10th cycle) and a maximum value of 147 MN/m^2 (21.3 ksi). Comparison with the reference case of no initial loading, for which local stress cycled between 0 and 355 MN/m^2 (51.4 ksi), shows that beneficial initial loading produced an algebraic decrease of 208 MN/m^2 (30.1 ksi) in local stress.

The local stresses for detrimental initial loading are shown in figure 4. The first 10 cycles, corresponding to high loading, are similar to those in figure 3 but terminate with a tensile residual stress of approximately 207 MN/m^2 (30 ksi). However, the first tensile half-cycle at the second-load level produced local yielding and therefore reduced this residual stress. Subsequent behavior was elastic with local stresses cycling between 69.6 MN/m^2 (10.1 ksi) and 424 MN/m^2 (61.5 ksi). Comparison with the reference case indicates that the detrimental initial loading produced an algebraic increase of 69.6 MN/m^2 (10.1 ksi) in local stresses.

For the first 10 cycles, the peak stresses determined by the Neuber procedure are in close agreement with those determined by the companion-specimen procedure. The slight decrease in stresses from the 10th to the 50th cycle for the companion-specimen method is believed to be an experimental error. Such errors can be explained in terms of unequal zero drifts for the strain gages (ref. 13) used on the notched and companion specimens.

Local strains.- Local strains are presented in figures 5 and 6. Strains determined by both the companion-specimen and Neuber procedures decreased sharply during the first few cycles to reflect the strain-hardening behavior of the material. The Neuber procedure predicted appropriate trends for the strains, but, in general, numerical values were in poor quantitative agreement with the experimental data.

Comparison of experimental results beyond the 10th cycle with the reference case, for which local strain cycled between 0 and 0.5 percent, shows that local maximum and minimum strains were increased by beneficial initial loading and decreased by detrimental initial loading. It should be emphasized that loading-sequence effects cannot be anticipated from these changes in local strain. Therefore, fatigue-analysis methods based entirely on local strain behavior cannot predict loading-sequence effects in notched specimens.

6

Effect of Initial High Loads on Crack Initiation

Data from the crack-initiation tests on notched specimens are presented in table 1; only geometric mean lives are shown in figure 7. These results display the anticipated sequence effects relative to the case of no initial high load: termination of initial high loading after a tensile peak produced longer lives; whereas, termination after a compressive peak produced shorter lives. The mean life for beneficial initial loading was approximately four times the reference life, whereas the mean life for detrimental initial loading was approximately 0.5 times the reference life. (See table 1.)

Results from the fatigue tests with unnotched specimens to simulate both residual stress and high local strain effects are given in table 2 and figure 7. For the three loading sequences, the mean lives of the unnotched specimens were shorter than those of notched specimens. This behavior is consistent with the well-known notch-size effect, whereby notches have less effect on fatigue life than is indicated by K_T. Since this notch-size effect influenced the three cases in a similar manner, it does not invalidate conclusions drawn from these data.

The results in table 2 for unnotched specimens show that the mean life for beneficial initial loading was approximately five times that for the reference case which had no initial high loading; for detrimental initial loading, the fatigue life was approximately 0.6 times the reference life. These factors agree closely with the corresponding values of 4 and 0.5 for the lives determined with notched specimens. Therefore, the results correctly indicate the effects of loading sequence on fatigue life.

The fatigue tests with unnotched specimens to simulate only residual stress effects were conducted with the stress limits shown beyond the 10th cycle in figures 3 and 4. These stresses and the resulting lives are given in table 3 and plotted in figure 7. The mean life for beneficial initial loading is nearly nine times the reference life from table 2, and for detrimental initial loading, the fatigue life is approximately 0.9 times the reference life. Since these ratios are significantly larger than the corresponding values of 4 and 0.5 for the notched specimen, the sequence effects found with notched specimens could not be attributed solely to residual stresses, as is usually assumed.

The differences between the lives simulating only residual stress effects (diamond symbols) and those simulating the complete-sequence effects (square symbols) can be attributed to the effects of the 10 cycles of high local strain corresponding to the initial high loading. Furthermore, since these 10 cycles represent only a negligibly small portion of fatigue life, based on the linear-damage rule, these differences show that the initial high local strains intensify the fatigue damage during subsequent cycling at smaller strains, as suggested in reference 11.

The portions of the sequence effects attributable to residual stress and high local strain effects can be determined from the lives in tables 2 and 3 with the aid of figure 7. For beneficial initial loading, the residual stress increased life by 265 400 cycles (from A to B), but the local strain effect decreased life by 109 900 cycles (from B to C) — for a net increase of 155 500 cycles. For detrimental initial loading, the residual stress decreased life by 3400 cycles (from A to B'), and the local strain effect further decreased life by 9100 cycles (from B' to C') — for a total decrease of 12 500 cycles.

These two loading sequences illustrate the importance of both the residual stress effects and the damaging effects of high local strain cycles. Both effects should be considered so that loading-sequence effects can be predicted accurately.

CONCLUDING REMARKS

Loading-sequence effects on crack-initiation period were investigated for notched specimens under high-low two-step loading. The sequence effects, demonstrated by the crack-initiation behavior of notched aluminum-alloy specimens, were explained in terms of local stress-strain conditions at the notch root.

Local stresses and strains were determined by the Neuber procedure. To evaluate the accuracy of this procedure, local stresses and strains were also measured experimentally. The Neuber procedure produced accurate local stress results but inaccurate local strains. Thus, life estimates based on local strains calculated by the Neuber method will be subject to errors.

The sequence effects were shown to be simulated accurately by fatigue tests of unnotched specimens under local stress sequences determined for notched specimens. An analysis of the sequence effects revealed that they were not solely the result of local residual stresses, as is usually assumed. The high initial local strain cycles were shown to contribute significant fatigue damage. The sequence effects observed with notched specimens were interpreted as the combined effect of residual stresses and high local strain cycles.

Langley Research Center,
    National Aeronautics and Space Administration,
        Hampton, Va., September 22, 1971.

8

APPENDIX A

NEUBER PROCEDURE

The Neuber procedure is a "semianalytical" technique for determining cyclic local stress and strain at a notch root. The procedure was presented in reference 5 and has been shown to produce reasonably accurate results for the case of constant-amplitude loading on a notched specimen. (See ref. 7.)

The procedure is explained with the aid of figure 8. The fatigue-critical points for the notched specimen lie on the boundary of the hole at points c. In thin specimens, a state of nearly uniaxial stress exists at these symmetrically located points. The stress state produced in the unnotched specimen under an applied stress of σ is similar to that at points c. Therefore, an unnotched specimen can be used to represent the cyclic stress-strain behavior at points c by cyclically loading the unnotched specimen between limiting conditions for stresses and strains that occur at points c. These limiting conditions were calculated by the Neuber equation (ref. 6)

$$K_T^2 = K_\sigma K_\epsilon \tag{A1}$$

which relates stress- and strain-concentration factors to the elastic stress-concentration factor. This equation was rewritten in reference 7 as

$$\Delta\sigma_i = \frac{\left(K_T \Delta S_i\right)^2}{\Delta\epsilon_i E} \tag{A2}$$

where $\Delta\sigma_i$ and $\Delta\epsilon_i$ are the changes in local stress and strain corresponding to the ith monotonic excursion of nominal stress ΔS_i. Substituting into equation (A2) values of K_T and E for a given configuration and material and a value of ΔS_i for a given load cycle results in an equation with only $\Delta\sigma_i$ and $\Delta\epsilon_i$ as unknowns. A particular solution for this equation can be determined by plotting it together with a uniaxial stress-strain curve for the material. The intersection of the curve for this equation with the stress-strain curve provides values of $\Delta\sigma_i$ and $\Delta\epsilon_i$ which satisfy equation (A2) and are also consistent with the stress-strain behavior of the material.

The cyclic application of this procedure is explained for the typical first cycle of nominal stress shown in figure 8. This cycle has been divided into monotonic excursions of nominal stress, and each excursion has been labeled. Equation (A2) has been evaluated for K_T, E, and ΔS_1 and is plotted as the dashed curve in the first quadrant of the sketch. This curve represents the locus of maximum values of local stress and strain corresponding to ΔS_1. An unnotched specimen was loaded in uniaxial tension to obtain

9

the stress-strain curve OA. Point A corresponds to the intersection of the curves and therefore represents the only combination of $\Delta\sigma_1$ and $\Delta\epsilon_1$ that satisfies equation (A2) and is also consistent with the stress-strain curve OA. Thus, point A represents the estimated maximum values of local stress and strain during the first quarter cycle. For the second excursion of nominal stress ΔS_2, point A was taken as the initial state. Accordingly, equation (A2) was plotted relative to point A for ΔS_2, as shown in the third quadrant. The unnotched specimen was unloaded from point A and loaded into compression until the resulting stress-strain curve intersected this limiting curve corresponding to ΔS_2. The intersection point B represents the estimate for the minimum values of local stress and strain for this cycle of nominal stress. The local stress-strain curves for cycling beyond the first cycle were determined by applying this procedure repeatedly to find the extreme points for each cycle. A typical recording is shown in figure 9 for three loading cycles.

Residual stresses and strains were found by a procedure also illustrated in figure 8. For the nominal stress cycle in this figure, equation (A2) was plotted relative to point A with $\Delta S_i = \Delta S_1$. The intersection of this curve and curve AB established the half-cycle residual stress and strain, point R_1, for the unloading excursion ΔS_1. As demonstrated with point R_2, subsequent residual conditions were determined by repeating this procedure for each unloading excursion.

APPENDIX B

COMPANION-SPECIMEN PROCEDURE

The companion-specimen procedure is an experimental technique for determining local cyclic stresses and strains at a notch. The method, as first presented in reference 10, was based on local strain measurements made while the load on the notched specimen was slowly cycled. This local strain sequence was then slowly reproduced under uniaxial tension in an unnotched companion specimen to duplicate the corresponding stresses. The sequence of stresses found in this manner was assumed to be a close approximation to the local stresses at the notch.

For the present study, this procedure was automated so that local stresses were determined in real time. A strain-coupled servocontrol shown in figure 10 was used to test simultaneously the notched and unnotched specimens. The control system shown on the left was used to load the notched specimen cyclically. The output signal from small foil strain gages at the notch root was compared with the output signals from similar foil strain gages on the unnotched specimen. The difference between these signals was amplified and used to control the loading on the unnotched specimen. Thus, the closed-loop control system maintained strains in the unnotched specimen that were equal to those at the notch root.

Quantitative strain data were obtained from an extensometer on the unnotched specimen. Loads applied to the two specimens were measured by load cells. Throughout a test the nominal stress S and the local stress σ were continuously plotted against local strain, as shown typically in figure 11.

REFERENCES

1. Miner, Milton A.: Cumulative Damage in Fatigue. J. Appl. Mech., vol. 12, no. 3, Sept. 1945, pp. A-159 – A-164.

2. Rosenthal, D.; and Sines, G.: Effect of Residual Stress on the Fatigue Strength of Notched Specimens. Proc. Am. Soc. Testing Mater., vol. 51, 1951, pp. 593-610.

3. Taira, Shuji; and Murakami, Yasunori: Residual Stresses Produced by Plastic Tension in Notched Plate Specimens and Fatigue Strength. Bull. JSME, vol. 4, no. 15, 1961, pp. 453-460.

4. Heywood, R. B.: The Influence of Pre-Loading on the Fatigue Life of Aircraft Components and Structures. C.P. No. 232, Brit. A.R.C., 1956.

5. Wetzel, R. M.: Smooth Specimen Simulation of Fatigue Behavior of Notches. J. Mater., vol. 3, no. 3, Sept. 1968, pp. 646-657.

6. Neuber, H.: Theory of Stress Concentration for Shear-Strained Prismatical Bodies With Arbitrary Nonlinear Stress-Strain Law. Trans. ASME, Ser. E: J. Appl. Mech., vol. 28, no. 4, Dec. 1961, pp. 544-550.

7. Crews, John H., Jr.: Elastoplastic Stress-Strain Behavior at Notch Roots in Sheet Specimens Under Constant-Amplitude Loading. NASA TN D-5253, 1969.

8. Comm. on Metric Pract.: ASTM Metric Practice Guide, NBS Handbook 102, U.S. Dep. Com., Mar. 10, 1967.

9. Howland, R. C. J.: On the Stresses in the Neighbourhood of a Circular Hole in a Strip Under Tension. Phil. Trans. Roy. Soc. (London), ser. A, vol. 229, no. 671, Jan. 6, 1930, pp. 49-86.

10. Crews, John H., Jr.: Local Plastic Stresses in Sheet Aluminum-Alloy Specimens With Stress-Concentration Factor of 2 Under Constant-Amplitude Loading. NASA TN D-3152, 1965.

11. Freudenthal, Alfred M.; and Heller, Robert A.: On Stress Interaction in Fatigue and a Cumulative Damage Rule. J. Aero/Space Sci., vol. 26, no. 7, July 1959, pp. 431-442.

12. Topper, T. H.; and Sandor, B. I.: Effects of Mean Stress and Prestrain on Fatigue Damage Summation. T. & A.M. Rep. No. 318 (Contract No. NOO-156-67-C-1875), Univ. of Illinois, Aug. 1968.

13. Gowda, C. B. Byre; and Topper, T. H.: Performance of Miniature Resistance Strain Gages in Low-Cycle Fatigue. Exp. Mech., vol. 10, no. 1, Jan. 1970, pp. 27N-38N.

TABLE 1.- EXPERIMENTALLY DETERMINED CRACK-INITIATION PERIODS

FOR NOTCHED SPECIMENS

Test condition	Crack-initiation periods, N_O, cycles	Geometric mean of crack-initiation periods, cycles
No initial high loading	90 700	115 600
	113 600	
	123 100	
	140 800	
Beneficial initial loading	233 000	458 900
	269 100	
	696 400	
	1 016 200	
Detrimental initial loading	61 800	62 900
	62 000	
	62 800	
	65 400	

TABLE 2.- CRACK-INITIATION PERIODS FROM SIMULATION OF

SEQUENCE EFFECTS BY USING UNNOTCHED SPECIMENS

Simulated test condition	Fatigue lives,[a] cycles	Geometric mean of fatigue lives, cycles
No initial high loading	19 200	35 100
	22 700	
	43 500	
	48 100	
	58 400	
Beneficial initial loading	140 000	190 600
	181 000	
	273 300	
Detrimental initial loading	17 300	22 600
	23 100	
	28 800	

[a] Used as estimates for crack-initiation periods for notched specimens.

TABLE 3.- CRACK-INITIATION PERIODS FROM SIMULATION OF RESIDUAL

STRESS EFFECTS BY USING UNNOTCHED SPECIMENS

Test condition	Maximum stress		Minimum stress		Fatigue lives, cycles	Geometric mean of fatigue lives, cycles
	MN/m^2	ksi	MN/m^2	ksi		
Beneficial initial loading	147	21.3	-208	-30.1	270 900	300 500
					276 900	
					361 700	
Detrimental initial loading	424	61.5	69.6	10.1	28 300	31 700
					32 400	
					34 600	

14

302.3 mm
(11.90 in.)

889 mm
(35.0 in.)

50.8 mm
(2.00 in.)

Rolling
direction

(a) Notched specimen.

71 mm
(2.8 in.)

Straight
section

25.4 mm
(1.00 in.)

20.3 mm
(0.80 in.)

279 mm
(11.0 in.)

(b) Unnotched specimen.
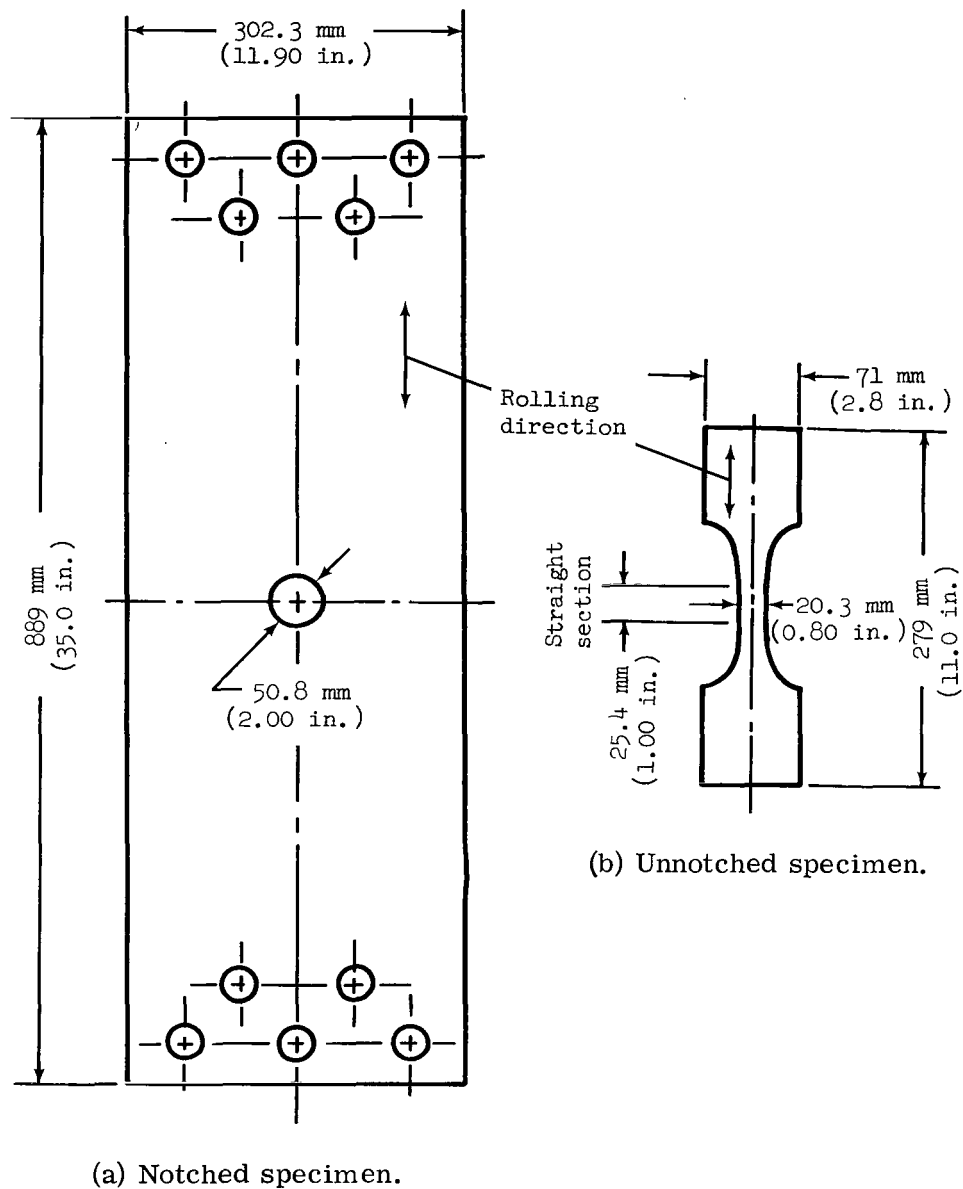
Figure 1.- Specimen configurations and dimensions. Material, 2024-T3 aluminum
alloy; thickness, 3.96 mm (0.156 inch).
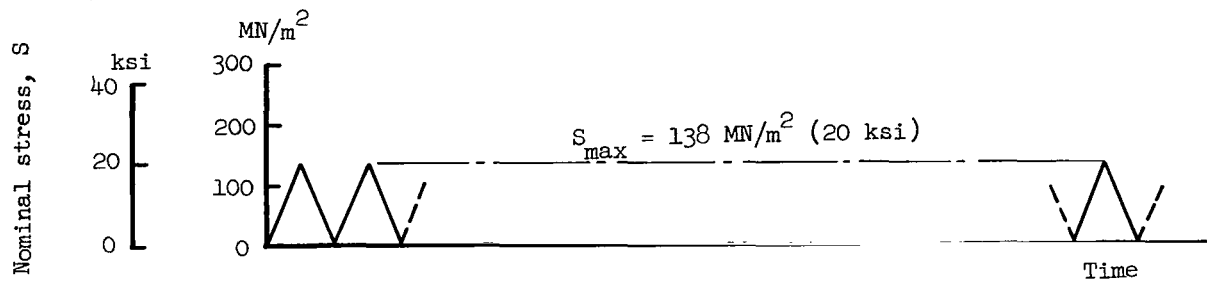
(a) No initial high loading.
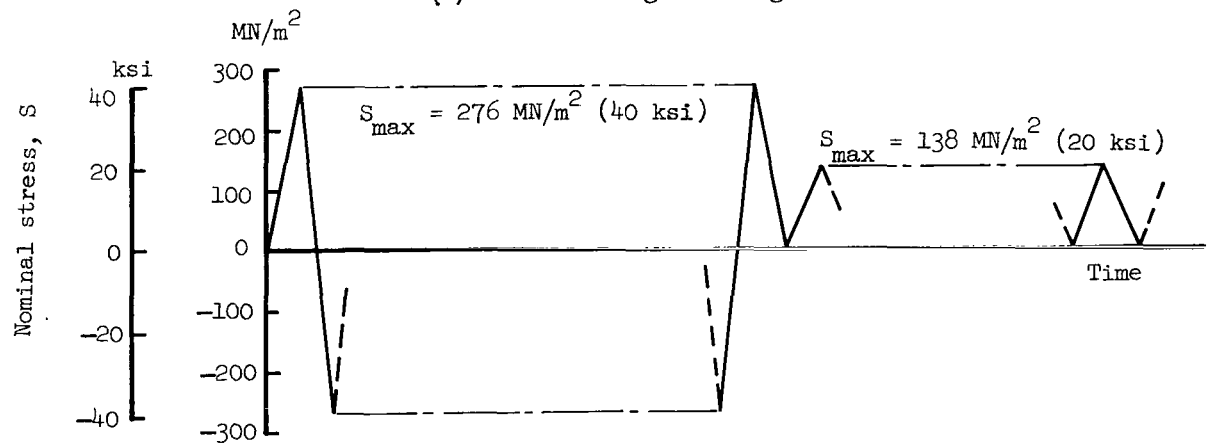
(b) Beneficial initial loading.
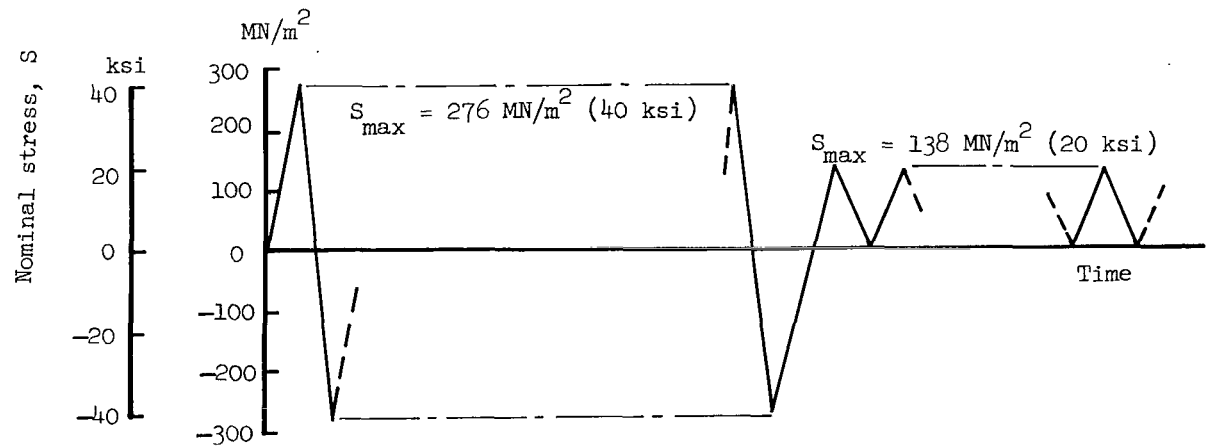
(c) Detrimental initial loading.

Figure 2.- Loading sequences for notched specimens.
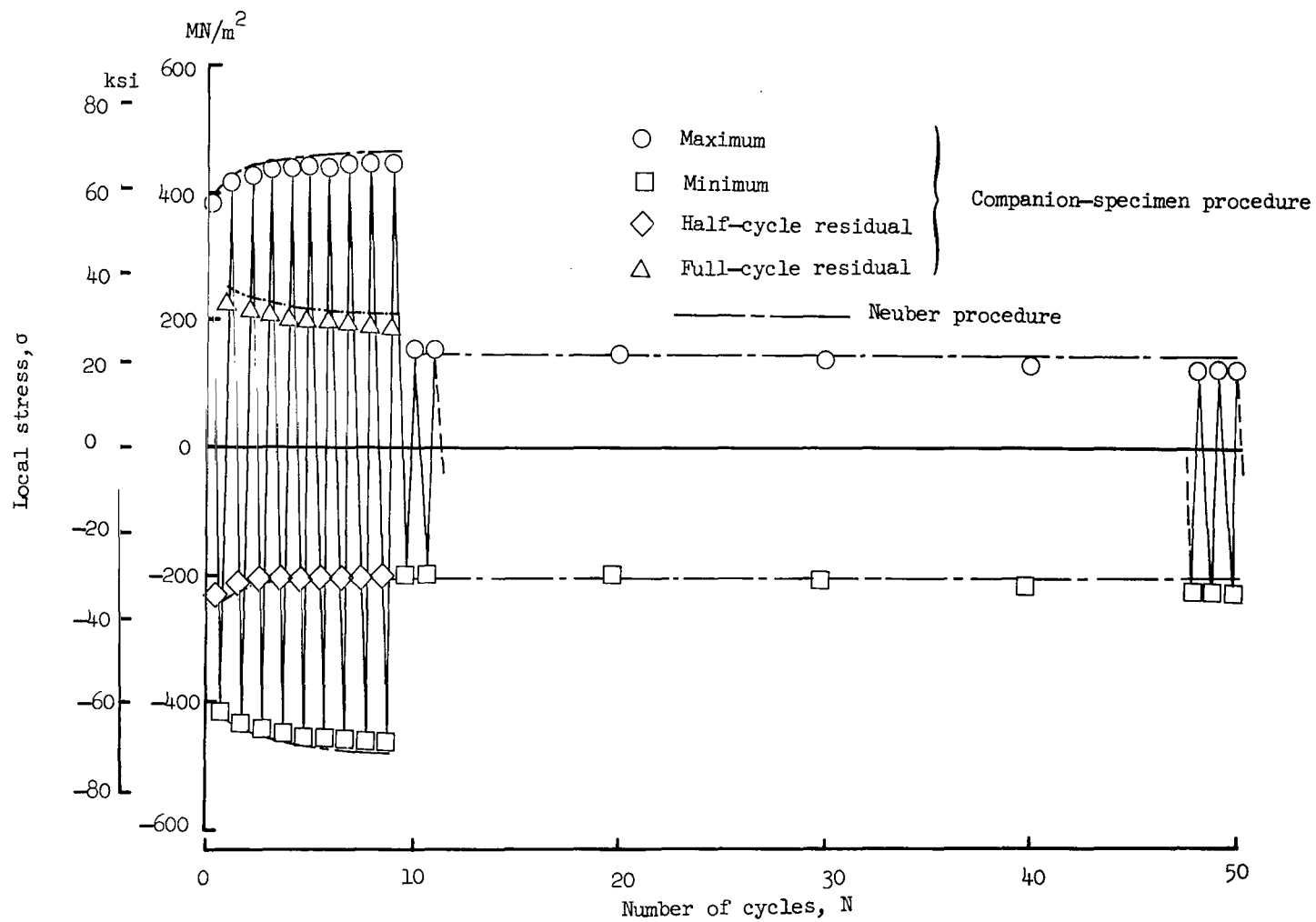
Figure 3.- Local stress for beneficial initial loading.
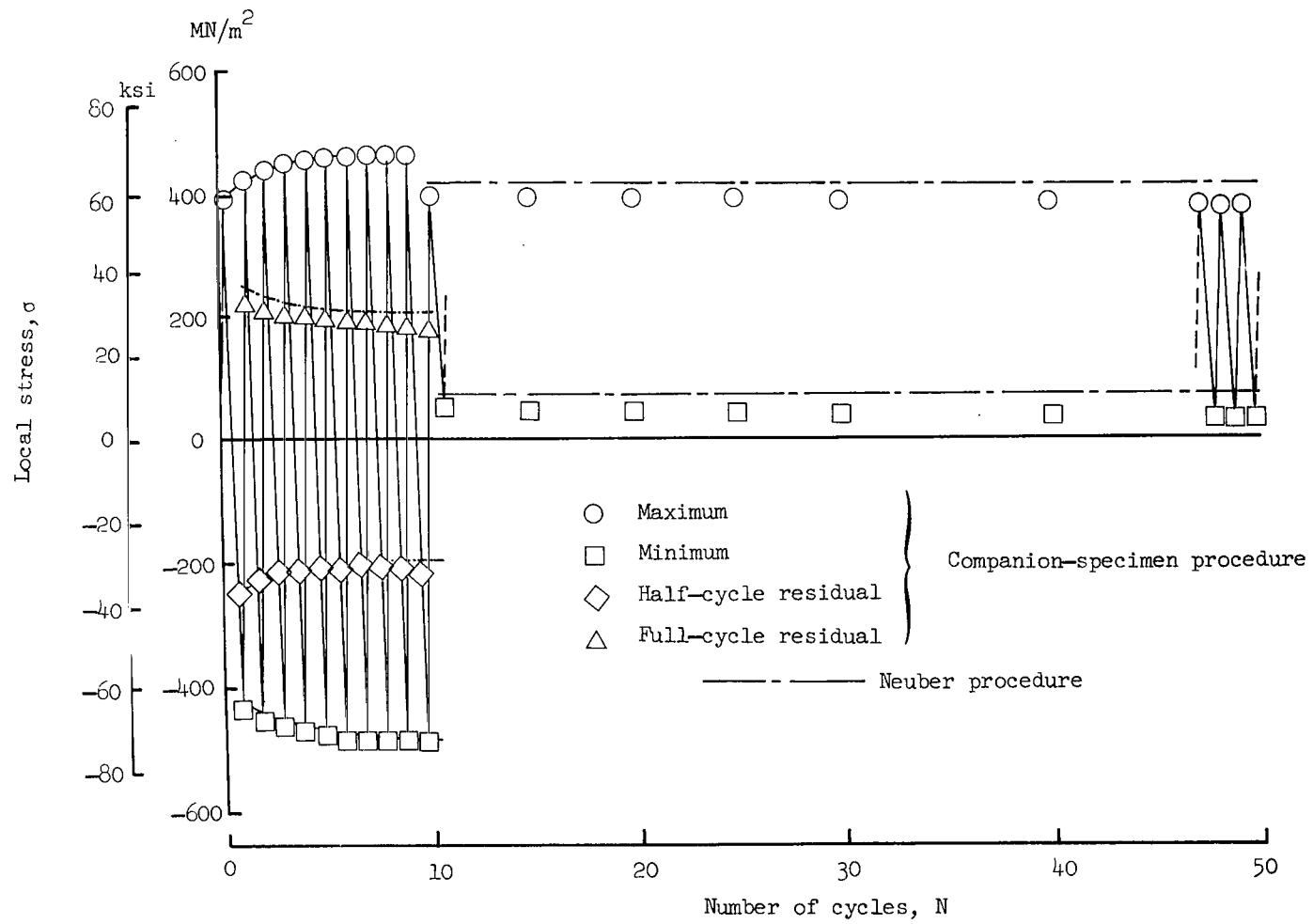
Figure 4.- Local stress for detrimental initial loading.
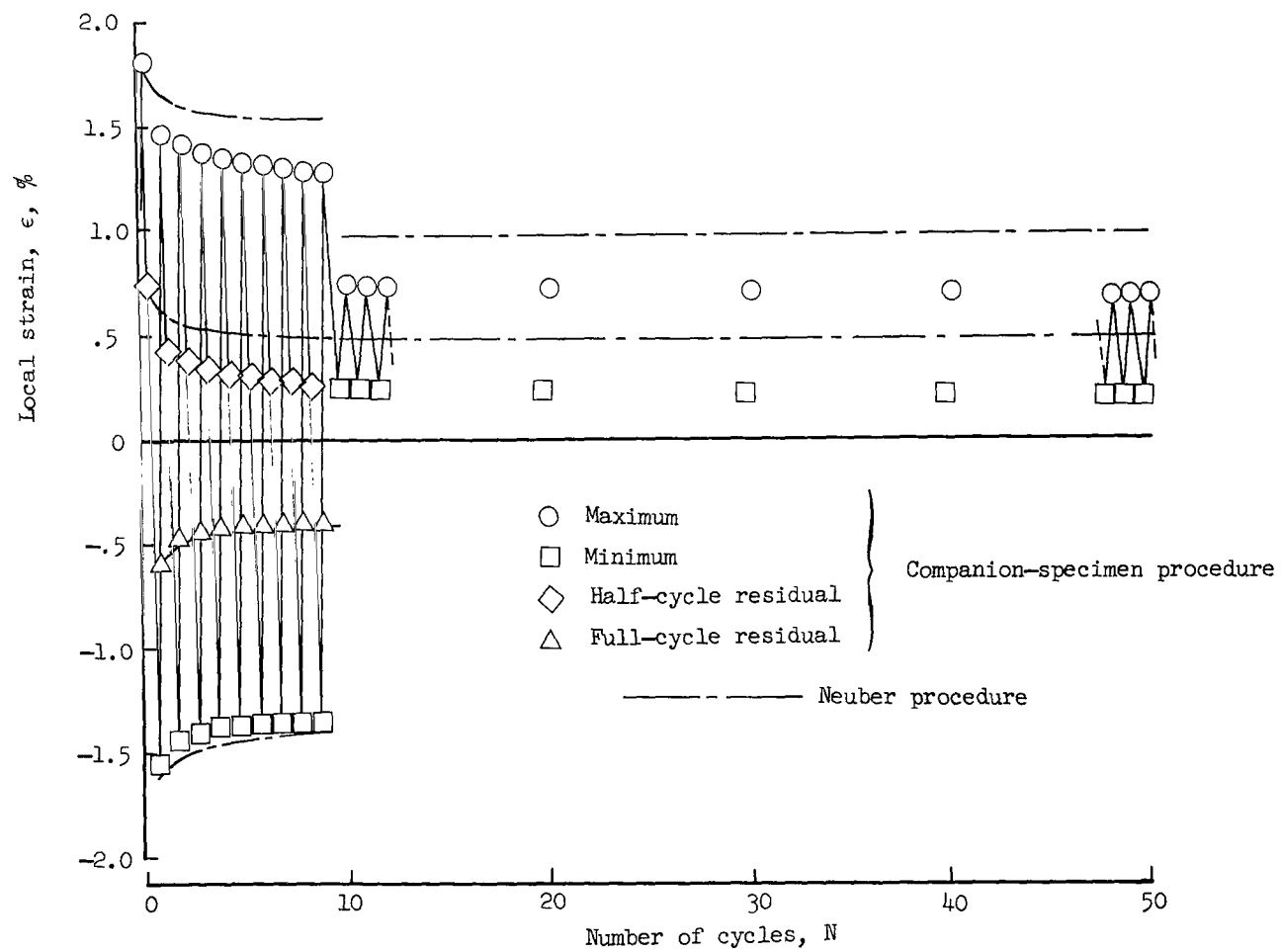
Figure 5.- Local strain for beneficial initial loading.
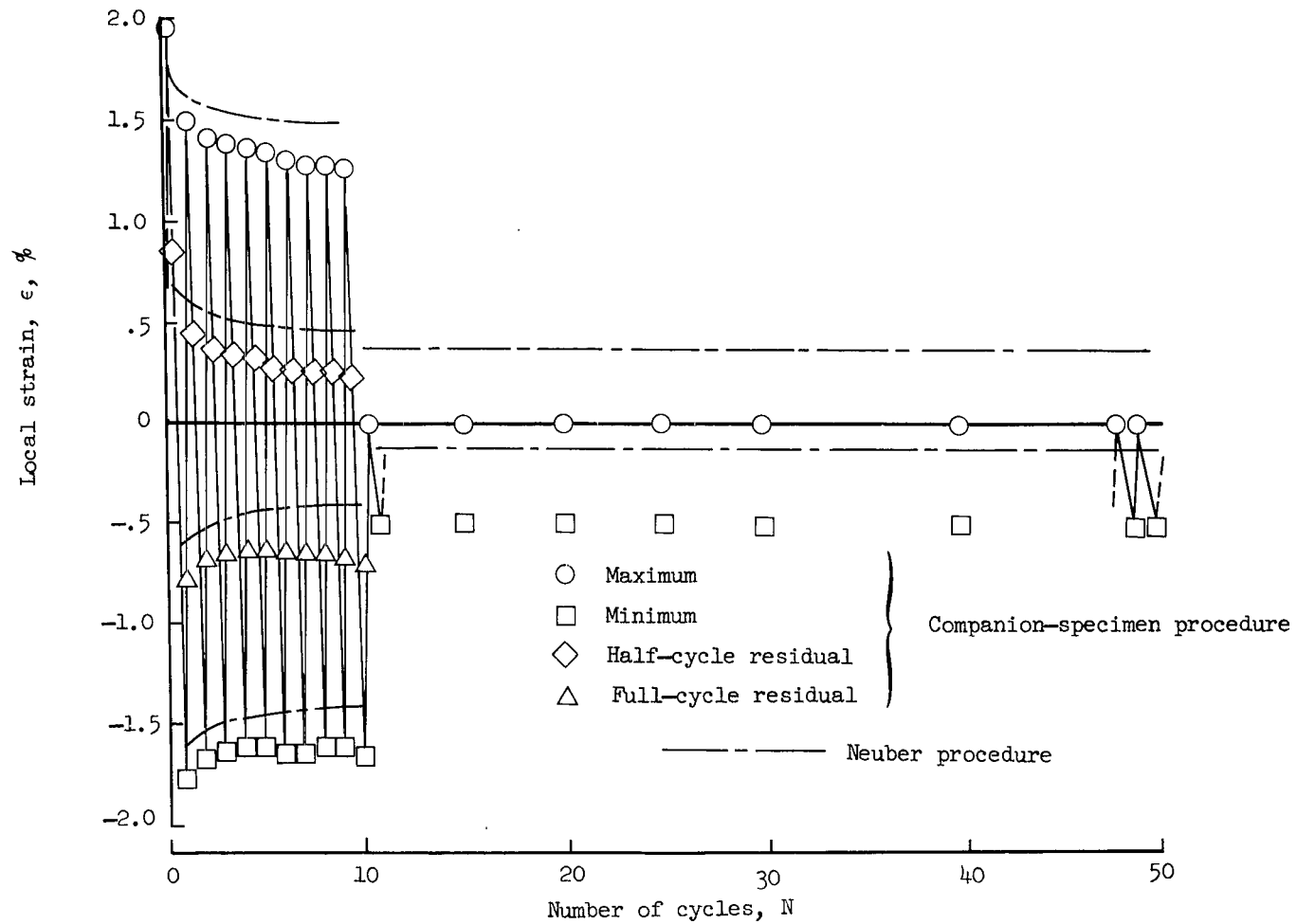
Figure 6.- Local strain for detrimental initial loading.
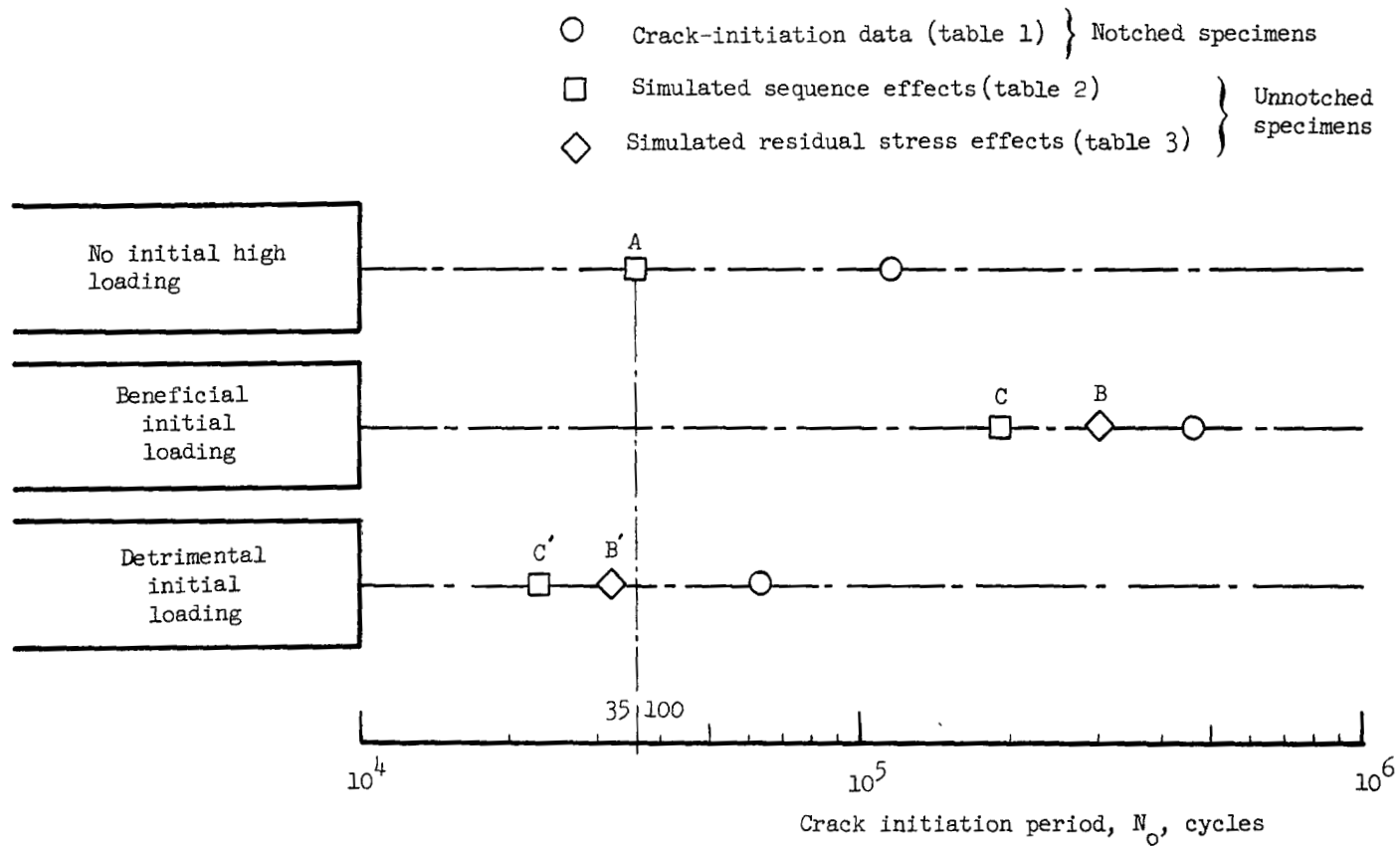
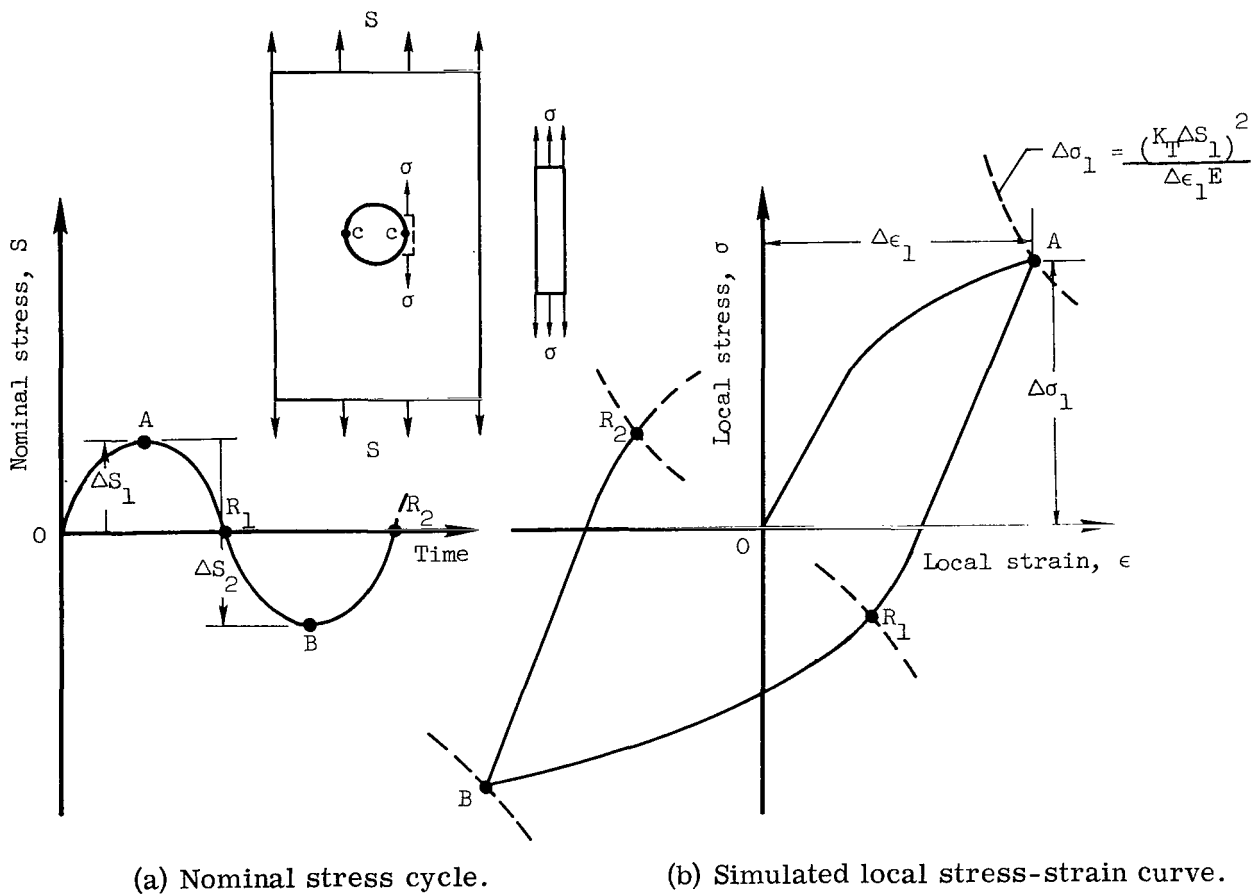Figure 7.- Crack-initiation periods. (Symbols represent geometric mean values.)

(a) Nominal stress cycle.   (b) Simulated local stress-strain curve.

Figure 8.- Nominal stress cycle and corresponding local stress-strain curve
by Neuber procedure.
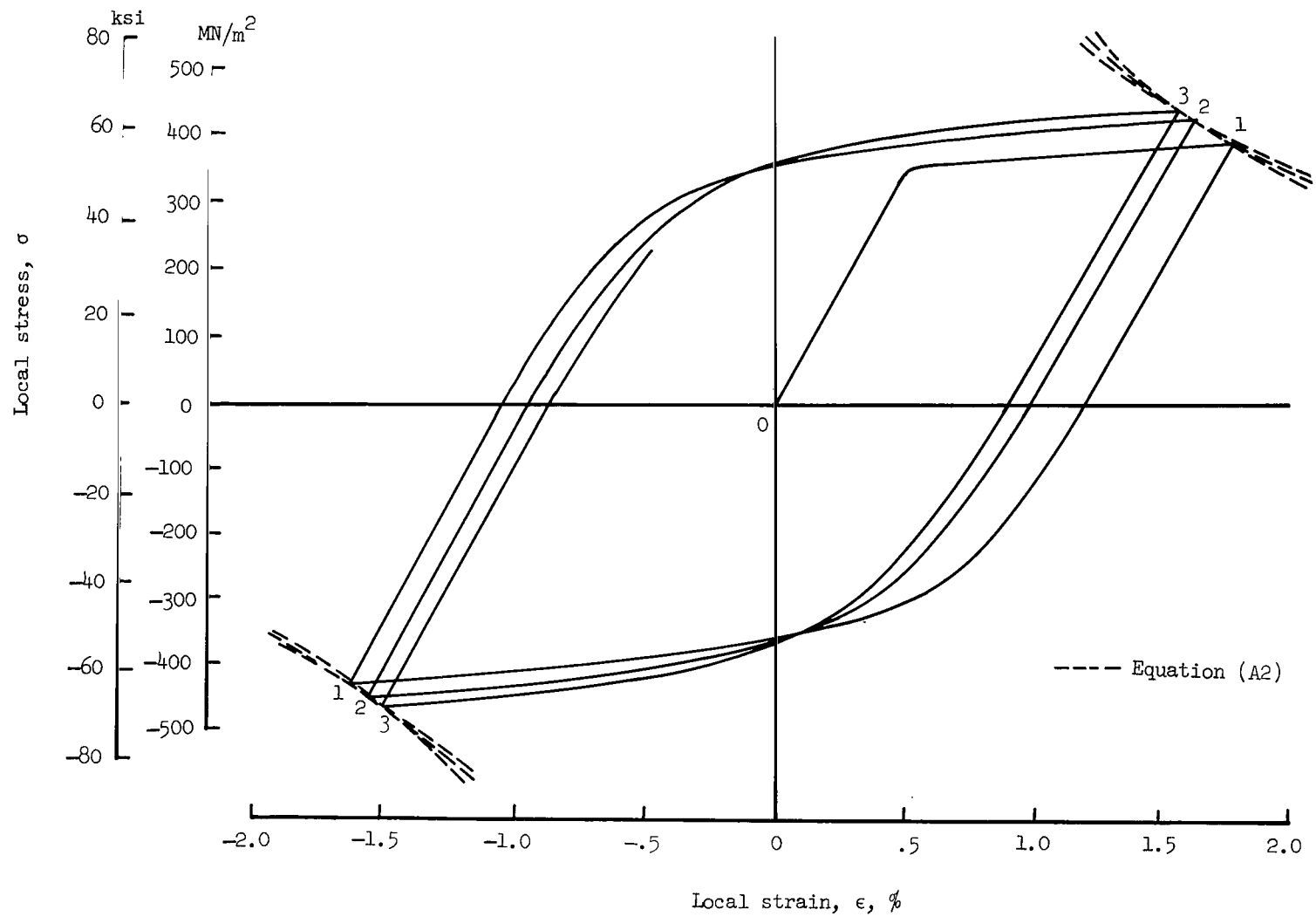
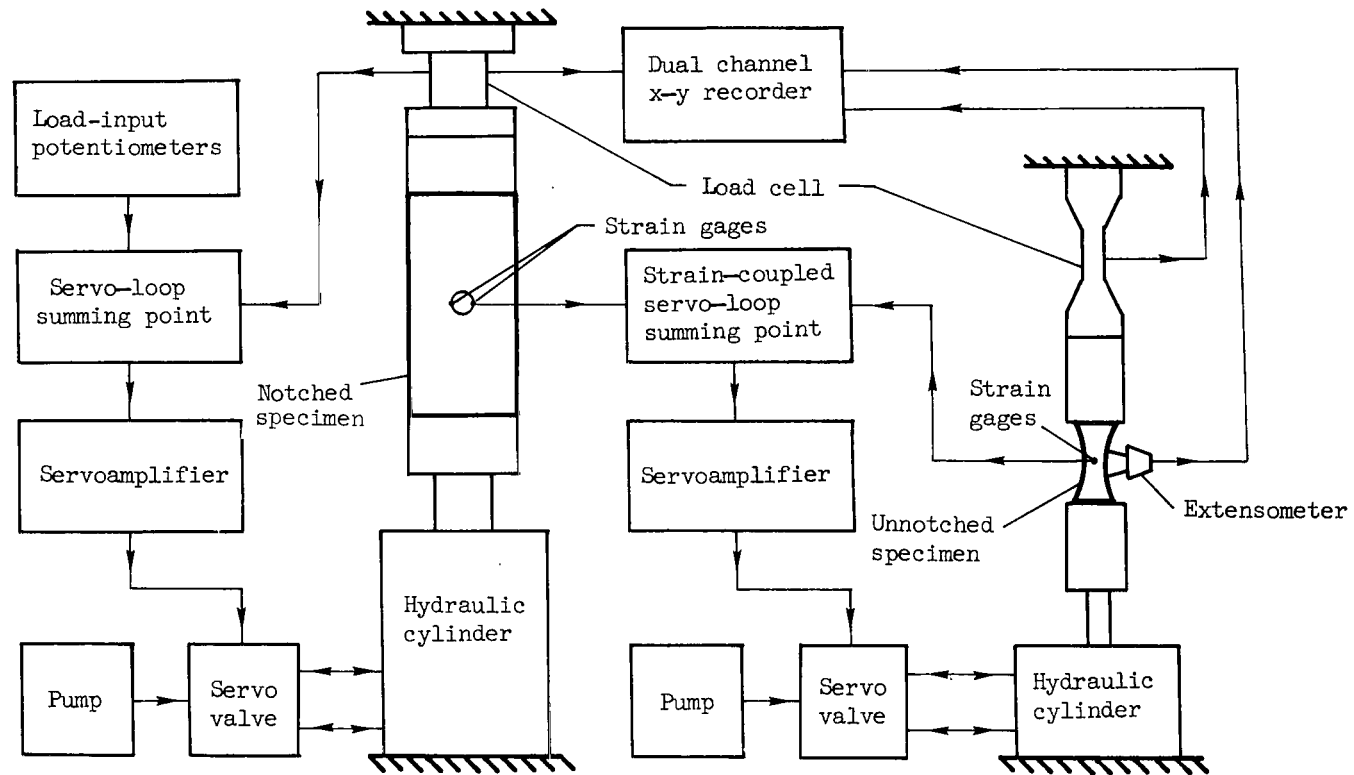Figure 9.- Typical recording from test by Neuber procedure.

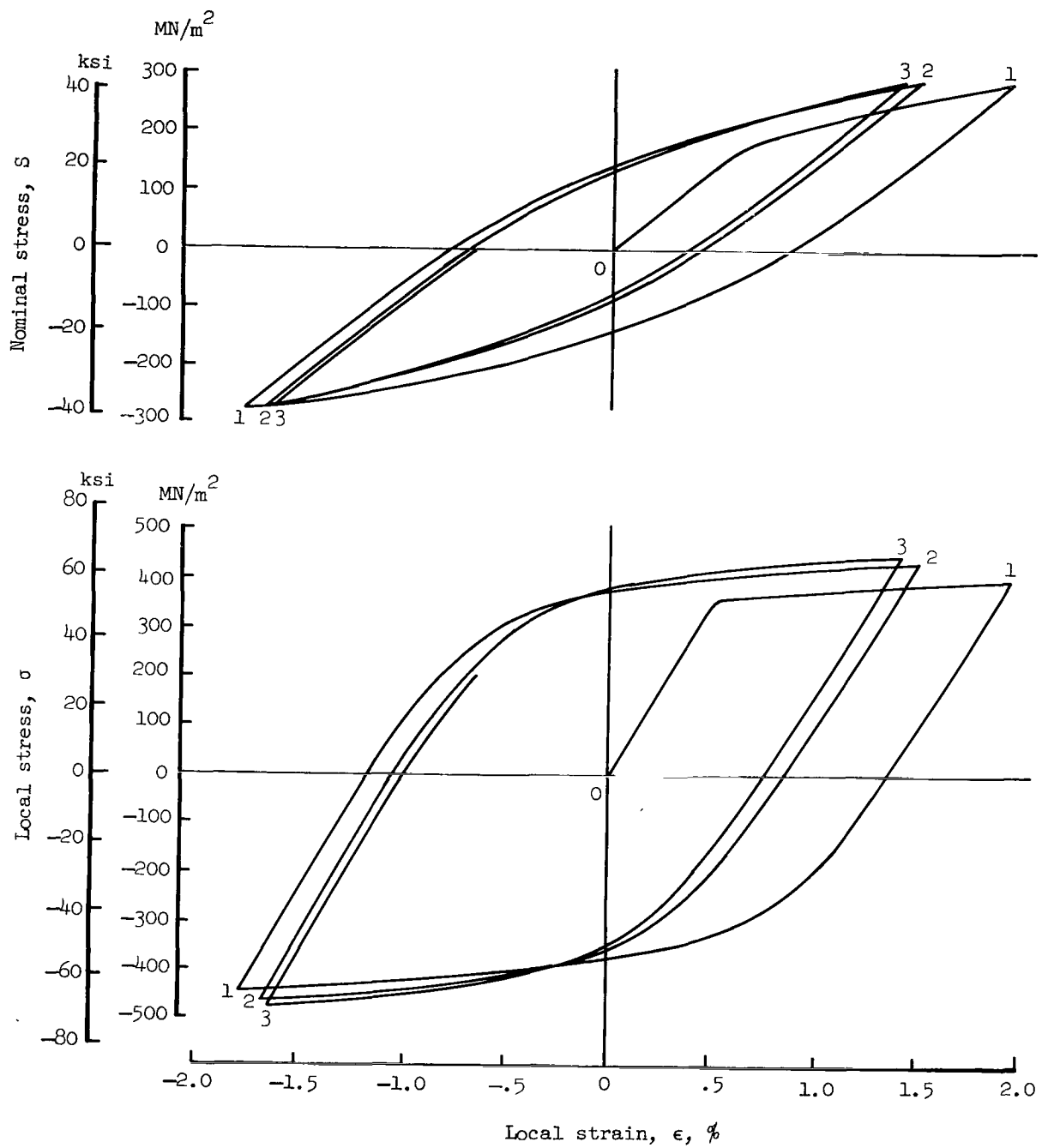Figure 10.- Block diagram of companion-specimen testing system.

Figure 11.- Typical recording from companion-specimen procedure.

"*The aeronautical and space activities of the United States shall be conducted so as to contribute . . . to the expansion of human knowledge of phenomena in the atmosphere and space. The Administration shall provide for the widest practicable and appropriate dissemination of information concerning its activities and the results thereof.*"

—NATIONAL AERONAUTICS AND SPACE ACT OF 1958

NASA SCIENTIFIC AND TECHNICAL PUBLICATIONS

TECHNICAL REPORTS: Scientific and technical information considered important, complete, and a lasting contribution to existing knowledge.

TECHNICAL NOTES: Information less broad in scope but nevertheless of importance as a contribution to existing knowledge.

TECHNICAL MEMORANDUMS: Information receiving limited distribution because of preliminary data, security classification, or other reasons.

CONTRACTOR REPORTS: Scientific and technical information generated under a NASA contract or grant and considered an important contribution to existing knowledge.

TECHNICAL TRANSLATIONS: Information published in a foreign language considered to merit NASA distribution in English.

SPECIAL PUBLICATIONS: Information derived from or of value to NASA activities. Publications include conference proceedings, monographs, data compilations, handbooks, sourcebooks, and special bibliographies.

TECHNOLOGY UTILIZATION PUBLICATIONS: Information on technology used by NASA that may be of particular interest in commercial and other non-aerospace applications. Publications include Tech Briefs, Technology Utilization Reports and Technology Surveys.

Details on the availability of these publications may be obtained from:

SCIENTIFIC AND TECHNICAL INFORMATION OFFICE

NATIONAL AERONAUTICS AND SPACE ADMINISTRATION
Washington, D.C. 20546